Loss of Apc allows phenotypic manifestation of the transforming properties of an endogenous K-*ras* oncogene *in vivo*

Owen J. Sansom*†, Valerie Meniel‡, Julie A. Wilkins*, Alicia M. Cole*, Karin A. Oien*, Victoria Marsh‡, Thomas J. Jamieson*, Carmen Guerra§, Gabrielle H. Ashton*, Mariano Barbacid§, and Alan R. Clarke‡

*Beatson Institute for Cancer Research, Glasgow G61 1BD, United Kingdom; ‡School of Biosciences, University of Cardiff, Cardiff CF10 3US, United Kingdom; and §Centro Nacional de Investigaciones Oncológicas, E-28029 Madrid, Spain

Edited by Bert Vogelstein, The Sidney Kimmel Comprehensive Cancer Center at Johns Hopkins, Baltimore, MD, and approved July 26, 2006 (received for review May 19, 2006)

Oncogenic mutations in the K-*ras* gene occur in ≈50% of human colorectal cancers. However, the precise role that K-*ras* oncogenes play in tumor formation is still unclear. To address this issue, we have conditionally expressed an oncogenic K-*ras*^{V12} allele in the small intestine of adult mice either alone or in the context of Apc deficiency. We found that expression of K-*ras*^{V12} does not affect normal intestinal homeostasis or the immediate phenotypes associated with Apc deficiency. Mechanistically we failed to find activation of the Raf/MEK/ERK pathway, which may be a consequence of the up-regulation of a number of negative feedback loops. However, K-*ras*^{V12} expression accelerates intestinal tumorigenesis and confers invasive properties after Apc loss over the long term. In renal epithelium, expression of the oncogenic K-*ras*^{V12} allele in the absence of Apc induces the rapid development of renal carcinoma. These tumors, unlike those of intestinal origin, display activation of the Raf/MEK/ERK and Akt signaling pathways. Taken together, these data indicate that normal intestinal and kidney epithelium are resistant to malignant transformation by an endogenous K-*ras* oncogene. However, activation of K-*ras*^{V12} after Apc loss results in increased tumorigenesis with distinct kinetics. Whereas the effect of K-*ras* oncogenes in the intestine can been observed only after long latencies, they result in rapid carcinogenesis in the kidney epithelium. These data imply a window of opportunity for anti-K-ras therapies after tumor initiation in preventing tumor growth and invasion.

colorectal cancer | renal carcinoma | Wnt signaling

Although the molecular genetic events that occur in colorectal cancer have been known for many years, the selective advantage conferred by these mutations has remained unclear (1, 2). Of these mutations, inactivation of Apc is the most frequent and appears to be the key early event initiating colorectal cancer (3). Recent *in vivo* studies using inducible gene deletion have allowed the precise function of Apc in the adult intestine to be defined (4). These studies have implicated two major functions of Apc in facilitating tumor suppression, namely controlling differentiation and migration.

K-*ras* is mutated in ≈40–50% of colorectal tumors at a relatively early stage of the carcinogenic process and, despite extensive research, the primary reason for this high frequency remains unclear (5). Ras proteins are prototypic small GTPases that act as molecular switches, transducing signals from the cell surface (from receptor and nonreceptor tyrosine kinases and G protein-coupled receptors) to the nucleus (5). The most studied downstream effector pathways are the mitogenic Raf-MEK-ERK pathway and the survival phosphatidylinositol 3-kinase pathway. *In vitro* studies have shown that oncogenic K-*ras* is required for proliferation, cytoskeleton organisation, adhesion, motility, and invasion of colorectal cancer cells. In these studies, activation of the downstream Raf-MEK-ERK pathways has been demonstrated, and inhibitors to this pathway have been shown to suppress the phenotypes induced by oncogenic K-*ras* (6).

To address the role of oncogenic K-*ras* *in vivo*, a number of strategies have been used. Most have relied on transgenic overexpression of oncogenic K-*ras* mutants (7). A key difficulty in interpreting these studies is that K-*ras* is normally mutated but not overexpressed in tumors. Thus, overexpression of oncogenic K-*ras* may yield very different phenotypes to simple mutation. When overexpressed from the villin promoter, mice developed tumors from 8 months of age, although no effects were seen on normal epithelium (7). As with *in vitro* studies, activation of Raf-MEK-ERK was observed in both normal and adenomatous tissue. In contrast, expression of oncogenic K-*ras* from the fatty acid-binding protein promoter only resulted in a proapoptotic phenotype in the context of a simian virus 40 T antigen transgene. In this study, the lack of phenotype mirrored an inability to see up-regulation of Raf-MEK-ERK signaling (8).

More sophisticated mouse models have been designed in which mutant alleles have been knocked in at the endogenous locus. Moreover, these mutant alleles have been designed so their expression can be controlled in a spatial and temporal manner using tissue-specific Cre and inducible Cre transgenic strains. One of these models involves the expression of an oncogenic K-*ras* allele under the control of a floxed STOP transcriptional cassette (9, 10). This oncogenic k-*ras* allele remains transcriptionally silent until the STOP is removed by a Cre recombinase. These models not only offer the advantage of the controlled expression of the desired knocked-in mutation, but the fact that conditional knockin allele is expressed from its endogenous promoter (9, 10).

These models have been used to demonstrate that endogenous K-*ras* oncogenes, activated in different tissues and at different times during embryonic or postnatal development, can induce myeloproliferative disease and carcinomas in various tissues including lung, pancreas, and ovaries (9–12). So far, there are no reports for a role of endogenous K-*ras* oncogenes in intestinal or colon tumors. Apc^{min} mice carrying an oncogenic K-*ras* allele whose expression required spontaneous recombination failed to display any phenotype significantly distinct of the Apc^{min} strain (9). Whether these observations were caused by a lack of synergy between the Apc and K-*ras* mutations or the low percentage of cells expressing the oncogenic K-*ras* allele could not be determined.

Here, we define the role of an endogenous K-*ras* oncogene in the adult intestine by using an inducible cre-lox approach. We show that although expression of the oncogenic K-*ras* allele has little or no

Conflict of interest statement: No conflicts declared.

This paper was submitted directly (Track II) to the PNAS office.

Abbreviations: PI, postinduction; IHC, immunohistochemistry; qRT-PCR, quantitative RT-PCR; RC, renal carcinoma.

†To whom correspondence should be addressed. E-mail: o.sansom@beatson.gla.ac.uk.

www.pnas.org/cgi/doi/10.1073/pnas.0604130103

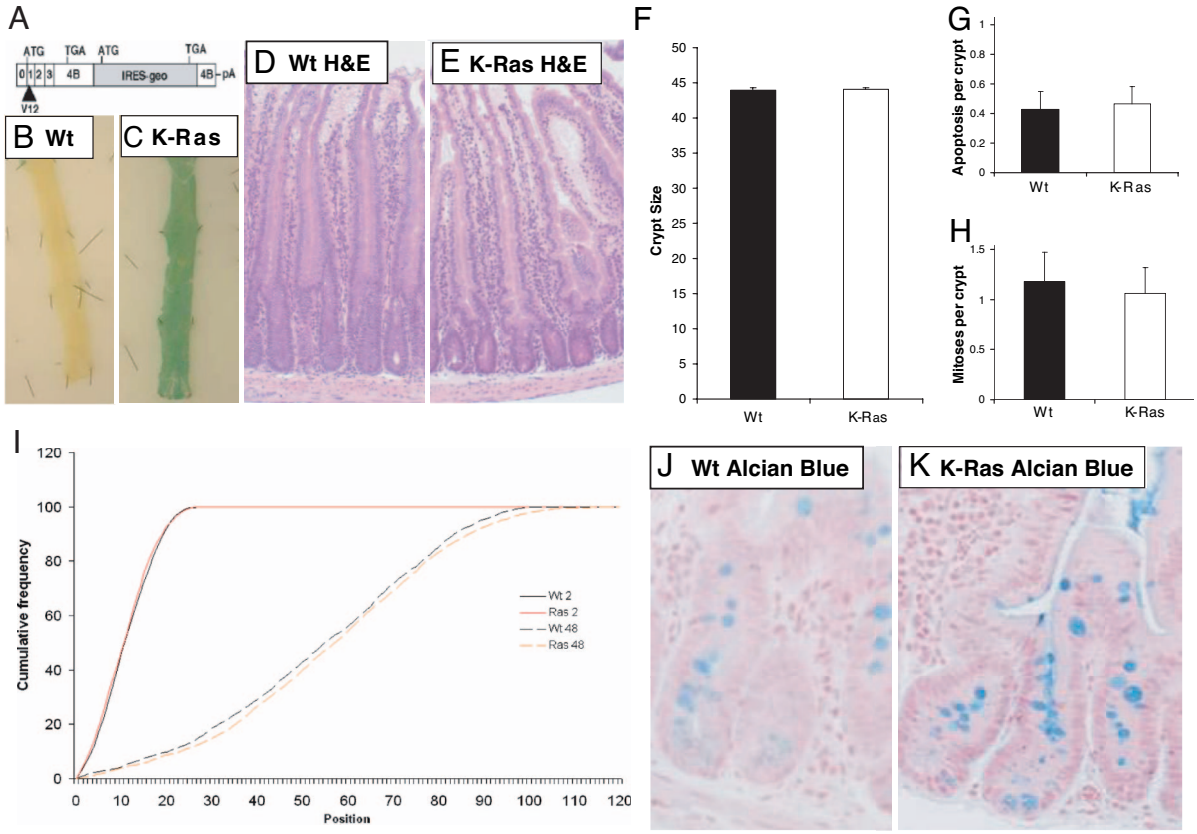

Fig. 1. Expression of oncogenic K-*ras*^{V12} has no impact on intestinal homeostasis. (*A*) Schematic diagram of the transcript derived from the conditional K-*ras*^{V12} allele. (*B* and *C*) Intestinal whole mounts showing β-gal expression in *AhCre*$^{+/T}$;*K-ras*$^{+/+}$ (WT) (*B*) and *AhCre*$^{+/T}$;*K-ras*$^{+/LSLV12}$ (K-Ras) (*C*). Note that the intestinal whole mount from the *AhCre*$^{+/T}$;*K-ras*$^{+/LSLV12}$ mouse is almost exclusively composed of LacZ-positive cells indicative of Cre-mediated K-*ras*^{V12} expression. (*D* and *E*) H&E-stained section from *AhCre*$^{+/T}$;*K-ras*$^{+/+}$ (WT) (*D*) and *AhCre*$^{+/T}$;*K-ras*$^{+/LSLV12}$ (K-Ras) (*E*) intestines. No gross changes were observed between these samples. (*F–H*) Graphs showing that crypt size, mitoses, and apoptotic indices are not altered between *AhCre*$^{+/T}$;*K-ras*$^{+/+}$ (WT) (filled bars) and *AhCre*$^{+/T}$;*K-ras*$^{+/LSLV12}$ (K-Ras) (empty bars) intestines. All of the above studies were performed 3 days after Cre induction. (*I*) Expression of oncogenic K-*ras*^{V12} does not affect migration or S-phase labeling. Mice were treated with BrdU and then culled either 2 or 48 h later at days 3 and 5 after recombination, respectively. The position of labeled cells was then scored relative to the base of the crypt and cumulative distribution plots generated. *AhCre*$^{+/T}$;*K-ras*$^{+/+}$ (WT) mice are indicated by black lines, and *AhCre*$^{+/T}$; *K-ras*$^{+/LSLV12}$ (K-Ras) mice are indicated by red lines. Solid lines, 2 h. Broken lines, 48 h. No differences were observed between the two genotypes at either time points ($P = 0.5$, Kolmorov–Smirnov). However, significant intestinal enterocyte migration was observed in both genotypes over the 48-h period of the experiment ($P > 0.01$ Kolmorov–Smirnov). (*J* and *K*) Alcian blue staining for goblet cells performed on *AhCre*$^{+/T}$;*K-ras*$^{+/+}$ (WT) (*J*) and *AhCre*$^{+/T}$;*K-ras*$^{+/LSLV12}$ (K-Ras) (*K*) intestines. No significant difference was found between genotypes ($P = 0.4$ Mann–Whitney). (Magnifications: ×40.)

effect on intestinal homeostasis or the immediate phenotype after Apc loss the K-*ras* oncogene does accelerate tumor formation and invasion. Importantly, we also show that expression of an endogenous K-*ras* oncogene in kidney cells accelerates the formation of renal carcinomas (RCs) after loss of Apc in the renal epithelium.

Results and Discussion

Activation of K-*ras* Does Not Alter Intestinal Homeostasis. We investigated whether expression of an oncogenic K-*ras*^{V12} allele would alter intestinal homeostasis. To this end, we intercrossed K-*ras*$^{(+/LSLV12)}$ mice bearing a conditional knocked-in K-*ras*^{V12} allele whose expression requires Cre-mediated elimination of a STOP transcriptional cassette (10) (Fig. 1*A*) to mice bearing the cytochrome p450 inducible AhCre transgene (13). After induction with β-naphthoflavone, the AhCre transgene delivers very high penetrance Cre-mediated recombination in both the intestine and liver, with subsequent expression of the oncogenic K-*ras*^{V12} allele in these tissues. This targeted allele also carries an IRES-betageo sequence that allows monitoring of successful Cre-mediated recombination through LacZ activity. Therefore, to confirm excision of the STOP cassette, we performed β-gal staining on intestinal whole mounts (Fig. 1 *B* and *C*). Nearly all intestinal cells stained positive for LacZ, indicating successful recombination of the knockin K-*ras*^{V12} allele throughout the intestine.

We next characterized the consequences of expressing the oncogenic K-*ras*^{V12} allele in the small intestine. Histological analysis revealed no major alterations in the architecture of the crypt-villus axis at 3 days after Cre induction. Crypt size, mitotic index, and levels of apoptosis were scored from these sections and found not to vary significantly between experimental and control tissue at day 3 postinduction (PI). For all comparisons $n \geq 3$ and Mann–Whitney U P values were ≥0.40 (Fig. 1 *F–H*). Levels of apoptosis were also confirmed independently with immunohistochemistry (IHC) staining for active caspase 3 (14) (data not shown). This failure to observe phenotypic change was consistently observed in mice up to 180 days after Cre induction.

Given previous data suggesting that oncogenic activation of K-ras may alter migration of cells, we determined whether cells expressing the oncogenic K-*ras*^{V12} allele were able to migrate normally along the crypt-villus axis. This "migration" refers to the upward displacement of intestinal epithelial cells and thus differs from classical cell migration. Mice at day 3 PI were injected with BrdU and killed after 2 or 48 h. Comparison of the distribution of BrdU-positive cells along the axis allows an assessment of the degree of movement along the crypt-villus

axis. As shown in Fig. 1*I*, cells expressing K-*ras*^{V12} showed a normal migration pattern between 2 and 48 h postlabeling compared with controls (Kolmogorov-Smirnov test, $P = 0.5$). The 2-h BrdU labeling experiment described above demonstrated that cells expressing oncogenic K-*ras*^{V12} proliferated normally, and that the location and size of the proliferative compartment within the crypt did not differ from controls ($P = 0.4$, Kolmogorov-Smirnov).

The presence and correct localization of all differentiated intestinal cell lineages was confirmed by use of specific stains or IHC against markers of the differentiated cell types. Alcian blue staining for goblet cells showed that there were similar numbers of goblet cells (Fig. 1 *H–J*); Grimelius staining showed that there was no significant change in the number of enteroendocrine cells (for all comparisons $n \geq 3$ and Mann–Whitney *U P* values were ≥0.39). Antilysozyme staining for paneth cells and antivillin staining for villus enterocytes also revealed no gross change in the number or localization of these cell types (data not shown).

Activation of K-*ras* Does Not Alter the Levels of Proliferation or Apoptosis After Apc Loss. In colorectal cancer, K-*ras* mutations occur after *Apc* mutations, so we next examined whether Cre-mediated expression of oncogenic K-*ras*^{V12} affected the immediate phenotypes of Apc deficiency. This was achieved by intercrossing *AhCre*$^{+/T}$, K-*ras*$^{+/LSLV12}$ animals with *Apc*$^{fl/fl}$ mice bearing a loxP flanked *Apc*^{580} allele (15). The resulting *AhCre*$^{+/T}$, K-*ras*$^{+/LSLV12}$, *Apc*$^{fl/fl}$ mice were then induced with β-naphthoflavone.

Histological analysis revealed that K-*ras*^{V12} expression had little impact on the previously reported phenotypes of *Apc* deficiency (4) (Fig. 4 *B* and *C*, which is published as supporting information on the PNAS web site). Crypt size, mitotic index, and levels of apoptosis all were increased compared with WT mice but were indistinguishable to that of *Apc*-deficient mice (for all comparisons $n \geq 3$ and Mann–Whitney *U P* values were ≥0.40) (Fig. 4 *D–F*). IHC for BrdU and Ki67 showed K-*ras*^{V12} expression did not increase levels of cell turnover, with proliferation independent of position in both genotypes. Likewise, K-*ras*^{V12} expression did not significantly alter the number of enteroendocrine cells, the mislocalization of paneth cells, or the reduction in villin expression after Apc loss (data not shown). However, there was significant rescue in the number of goblet cells after *Apc* loss [34 ± 14 (*Apc*$^{fl/fl}$) vs. 113 ± 10 (*K-ras*$^{(+/LSLV12)}$, *Apc*$^{fl/fl}$), $P = 0.04$ Mann–Whitney, $n = 3$] (Fig. 4 *I–J*). Taken together, these data suggest that *Apc* loss alone is sufficient to induce the vast majority of changes that occur at the earliest stages of neoplasia and that K-*ras*^{V12} expression at these stages confers little, if any, additional phenotype.

Raf-MEK-ERK and Wnt Signaling Pathways Are Not Dysregulated After Expression of Oncogenic K-*ras*^{V12}. Given our failure to observe any phenotypic change after expression of the oncogenic K-*ras*^{V12} allele, we next investigated whether the Raf-MEK-ERK pathway was activated. IHC for P-MEK and P-ERK indicated that these phospho-proteins are normally present in the cytoplasm of intestinal enterocytes and that expression of oncogenic K-*ras*^{V12}, either alone or in the context of *Apc* deficiency, did not affect either the levels or the localization of these proteins (Fig. 5*a A–I*, which is published as supporting information on the PNAS web site). These observations provide a molecular explanation for our failure to see phenotypic changes after activation of K-*ras*^{V12} expression. These data also argue against the notion that Apc inhibits activation of the Raf-MEK-ERK pathway *in vivo*, as recently suggested (16). Interestingly, nuclear P-MEK and P-ERK were observed in goblet cell nuclei, suggesting that this pathway may be relevant to goblet cell differentiation (Fig. 5*aF*). This may also explain the partial rescue of goblet cell loss, which we report in *Apc*-deficient cells that express the oncogenic K-*ras*^{V12} allele.

We next investigated expression of cell-cycle proteins cyclin D1 and p21, which have also been reported to become up-regulated after expression of K-*ras* oncogenes (12). However, IHC showed no changes of localization or expression of either p21 or cyclin D1 after K-ras activation (data not shown). Previous studies have suggested that oncogenic K-*ras* may also activate Wnt signaling (17). Within the intestinal crypt, levels of Wnt signaling are crucial for the establishment of cell positioning, differentiation, and proliferation (4). We therefore examined expression of β-catenin after Cre-mediated expression of the oncogenic K-*ras*^{V12} allele in otherwise normal epithelium. No changes were observed in either the level or location of β-catenin in cells expressing oncogenic K-*ras*^{V12} as determined by IHC (Fig. 5*a K–L*). These data, in conjunction with the failure to see changes in crypt kinetics or up-regulation of the Wnt targets CD44 and C-Myc (WT vs. *K-ras*$^{(+/LSLV12)}$, 1.31- and 0.83-fold by quantitative RT-PCR (qRT-PCR), respectively, Mann–Whitney $P > 0.4$), argue that Wnt signaling was unaltered despite oncogenic K-*ras*^{V12} expression.

We also determined whether expression of the K-*ras*^{V12} allele altered Wnt signaling after Apc gene deletion. Irrespective of K-*ras*^{V12} expression status, β-catenin translocated to the nucleus (Fig. 5*a M* and *N*), causing transcriptional activation of the canonical Wnt target genes CD44 and C-Myc (WT vs. *Apc*$^{fl/fl}$, 6.72-fold, 1.88-fold, WT vs. *K-ras*$^{(+/LSLV12)}$, *Apc*$^{fl/fl}$ 5.33-fold, 2.72-fold changes, respectively by qRT-PCR). Wnt signaling was not accentuated after K-*ras*^{V12} expression in Apc-deficient cells with the levels of induction of CD44 and C-Myc unchanged (0.79- and 1.46-fold change, respectively by qRT-PCR, Mann–Whitney $P > 0.2$).

Up-Regulation of Negative Regulators of Raf-MEK-ERK Signaling. Previously we have shown that numerous negative feedback loops are activated after Apc loss *in vivo* (4). Thus, we observe up-regulation of Axin-2, Wisp1, Wif-1, and Frizzled 6 after Apc loss. However, in the absence of Apc, these proteins are unable to prevent dysregulated Wnt signaling (2) (Fig. 5*aM*). A different scenario exists after expression of the oncogenic K-*ras*^{V12} allele, as a number of studies have indicated that activation of the Ras signaling pathway can be attenuated through reducing the phosphorylation status of the downstream proteins Raf-MEK-ERK (18). Importantly, this has been the rationale behind developing kinase inhibitors to Raf and a number of other downstream effectors of Ras signaling.

To further explore the molecular consequences of oncogenic K-*ras*^{V12} expression, we performed microarray experiments using MOE430_2 chips comparing control and *AhCre*$^{+}$, K-*ras*$^{(+/LSLV12)}$ intestines. Using significance analysis of microarray analysis and a false discovery rate of 5% we identified a small number of changes specific to K-*ras*^{V12} expression. Of these, a number have previously been associated with Ras or G protein receptor signaling (Table 1, which is published as supporting information on the PNAS web site). Regulator of G protein signaling-5 (RGS5), a potential negative regulator of Ras signaling, was up-regulated in the array and confirmed by qRT-PCR to be 3-fold elevated after Cre-mediated induction of K-*ras*^{V12} expression. This protein was originally identified in a screen for regulators of G protein signaling and has been shown to attenuate ERK activation *in vivo* (19, 20).

The most studied phosphatases of the Raf-MEK-ERK pathway are the Dusp/MKP phosphatases. Our previous microarray analysis of Apc-deficient intestines had suggested that Dusp4/Mkp2 and Dusp9/Mkp4 were both up-regulated after Apc loss. To investigate this we performed IHC against Dusp4 after Apc loss and confirmed Dusp4 to be up-regulated immediately after Apc loss and to be independent of K-*ras* status (Fig. 6, which is published as supporting information on the PNAS web site). We also used qRT-PCR to confirm 5-fold up-regulation of Dusp9 after Apc loss, which again was independent of K-*ras*^{V12} expression. Previous studies have shown that K-*ras*-mediated transformation of pancreatic cells *in vitro* can be suppressed by cotransfection with vectors containing Dusp4 (21). Deregulation of Dusp4 and Dusp9 therefore provides

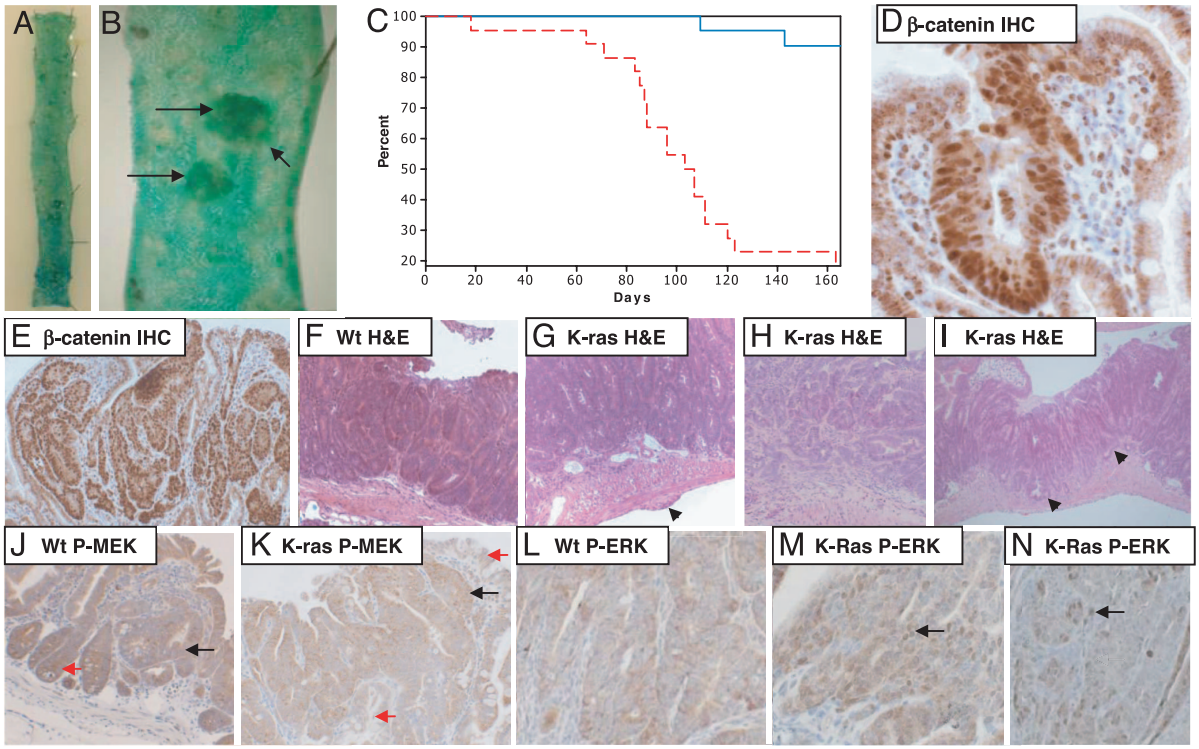

Fig. 2. Expression of endogenous K-*ras*^{V12} accelerates tumor growth and invasion within the intestine. (*A*) Intestinal whole mounts showing β-gal expression in *AhCre*$^{+/T}$, K-*ras*$^{+/LSLV12}$, *Apc*$^{+/fl}$ 150 days after Cre induction. (*B*) Close-up showing LacZ-positive blue intestinal adenomas. (*C*) Kaplan–Meier curve showing survival of *AhCre*$^{+/T}$, K-*ras*$^{+/LSLV12}$, *Apc*$^{+/fl}$ (red dashed line) and *AhCre*$^{+/T}$, K-*ras*$^{+/+}$, *Apc*$^{+/fl}$ (blue line) after Cre induction. Expression of oncogenic K-*ras*^{V12} rapidly accelerates tumorigenesis. (*D* and *E*) β-catenin relocalizes to the nuclei of all adenomatous cells in *AhCre*$^{+/T}$, K-*ras*$^{+/LSLV12}$, *Apc*$^{+/fl}$ tumors, indicating deregulation of the Wnt pathway. (*F*) H&E-stained section of an adenoma from *AhCre*$^{+/T}$, K-*ras*$^{+/+}$, *Apc*$^{+/fl}$ mouse. Note the lack of any signs of invasion. (*G*) Adenoma from *AhCre*$^{+/T}$, K-*ras*$^{+/LSLV12}$, *Apc*$^{+/fl}$ showing scarring on the outer surface of the intestine (denoted by arrows), which occurred frequently in *AhCre*$^{+/T}$, K-*ras*$^{+/LSLV12}$, *Apc*$^{+/fl}$ mice but was not seen in control *AhCre*$^{+/T}$, K-*ras*$^{+/+}$, *Apc*$^{+/fl}$ mice. In humans such external (serosal) thickening below a tumor is generally associated with adenocarcinomas rather than adenomas. (*H* and *I*) Adenocarcinoma from *AhCre*$^{+/T}$, K-*ras*$^{+/LSLV12}$, *Apc*$^{+/fl}$ showing invasion into the muscle wall (shown by arrows in *I*). (*J* and *K*) P-Mek staining of adenomas arising in a *AhCre*$^{+/T}$, K-*ras*$^{+/+}$, *Apc*$^{+/fl}$ mouse (*J*) and a *AhCre*$^{+/T}$, K-*ras*$^{+/LSLV12}$, *Apc*$^{+/fl}$ mouse (*K*). Note cytoplasmic P-Mek staining is more intense in the adenoma from the *AhCre*$^{+/T}$, K-*ras*$^{+/LSLV12}$, *Apc*$^{+/fl}$ mouse (black arrows) compared with surrounding normal mucosa (red arrows). This is not the case in the *AhCre*$^{+/T}$, K-*ras*$^{+/+}$, *Apc*$^{+/fl}$ adenomas (*J*). (*L–N*) P-ERK 1/2 staining of adenomas from *AhCre*$^{+/T}$, K-*ras*$^{+/+}$, *Apc*$^{+/fl}$ (*L*) and *AhCre*$^{+/T}$, K-*ras*$^{+/LSLV12}$, *Apc*$^{+/fl}$ (*M* and *N*). Note that nuclear P-ERK 1/2 was not observed in adenomas from the *AhCre*$^{+/T}$, K-*ras*$^{+/+}$, *Apc*$^{+/fl}$ mouse even in large adenomas (*L*). However, nuclear staining was evident in a number of adenomas from *AhCre*$^{+/T}$, K-*ras*$^{+/LSLV12}$, *Apc*$^{+/fl}$ mice (*M* and *N*). Black arrows shows nuclear staining in adenomas. Wt represents *AhCre*$^{+/T}$, K-*ras*$^{+/+}$, *Apc*$^{+/fl}$ and K-Ras represents *AhCre*$^{+/T}$, K-*ras*$^{+/LSLV12}$, *Apc*$^{+/fl}$. (Magnifications: *D–N*, ×400.)

a ready mechanism to explain the lack of additional phenotype we see after K-*ras*^{V12} expression.

Expression of K-*ras*^{V12} Accelerates Tumorigenesis and Causes Invasion After *Apc* Loss. After establishing that K-*ras*^{V12} expression has no detectable impact on the immediate consequences of *Apc* loss, we next investigated whether expression of this oncogenic allele could accelerate the appearance of adenomas. Cohorts of (*AhCre*$^{+/T}$, *K-ras*$^{+/+}$, *Apc*$^{+/+}$), (*AhCre*$^{+/T}$, *K-ras*$^{+/LSLV12}$, *Apc*$^{+/+}$), (*AhCre*$^{+/T}$, *K-ras*$^{+/+}$, *Apc*$^{+/fl}$), and (*AhCre*$^{+/T}$, *K-ras*$^{+/LSLV12}$, *Apc*$^{+/fl}$) mice were induced with β-naphthoflavone at weaning (3 × 80 mg/kg β-naphthoflavone i.p.). This protocol effectively renders the animals either WT or constitutively heterozygous for *Apc* from weaning, and additionally either WT or activated for K-*ras*. Cohorts were aged until they developed symptoms of intestinal neoplasia (anaemia, pale feet, hunching, and swollen abdomen). Fig. 2 *A* and *B* shows an intestinal whole mount of an *AhCre*$^{+/T}$, *K-ras*$^{+/LSLV12}$, *Apc*$^{+/fl}$ mouse at 150 days after induction of Cre expression stained for β-gal activity. LacZ staining was observed in both normal and adenomatous tissue throughout the intestine, consistent with high levels of Cre-induced expression of the conditional K-*ras*^{V12} allele. All adenomas were characterized by nuclear β-catenin, strongly implicating loss of the remaining Apc allele (Fig. 2 *D* and *E*).

Fig. 2*C* shows that expression of K-*ras*^{V12} rapidly accelerated intestinal tumorigenesis after *Apc* loss. By 165 days, 17 of 21 (81%) *AhCre*$^{+/T}$, *K-ras*$^{+/LSLV12}$, *Apc*$^{+/fl}$ animals had become symptomatic of disease and were culled because of the development of multiple intestinal tumors. Instead, only 2 of 20 (10%) *AhCre*$^{+/T}$, *K-ras*$^{+/+}$, *Apc*$^{+/fl}$ mice had a similar phenotype ($\chi^2 = 20.739$, df = 1, $P = 0.0001$). At death, there was no significant difference in tumor number or size (Mann–Whitney $P > 0.4$, $n = 18$ and $n = 6$), indicating that mice were being culled when they had a similar tumor burden.

As K-*ras* oncogenes had previously been associated with increased mobility of colorectal cancer cells *in vitro* (6), we investigated whether the invasive status of the tumors was altered in *AhCre*$^{+/T}$, *K-ras*$^{+/LSLV12}$, *Apc*$^{+/fl}$ mice. No adenocarcinomas were found in 100 tumors analyzed in *AhCre*$^{+/T}$, *K-ras*$^{+/+}$, *Apc*$^{+/fl}$ mice. These data consolidate data in the Apc$^{+/Min}$ mouse, which rarely, if ever, show progression to adenocarcinoma and do not show K-*ras* mutations. However 17 of 100 tumors arising in *AhCre*$^{+/T}$, *K-ras*$^{+/LSLV12}$, *Apc*$^{+/fl}$ double mutant mice showed morphological evidence of invasion into the smooth muscle and were classified as adenocarcinomas (Fig. 2 *F–I*). This significant increase in invasion ($\chi^2 = 18.579$, df = 1, $P = 0.001$) was observed despite the early onset of tumor formation in this cohort.

We next investigated whether this increased tumorigenesis was associated with activation of the Raf-MEK-ERK pathway. Previous

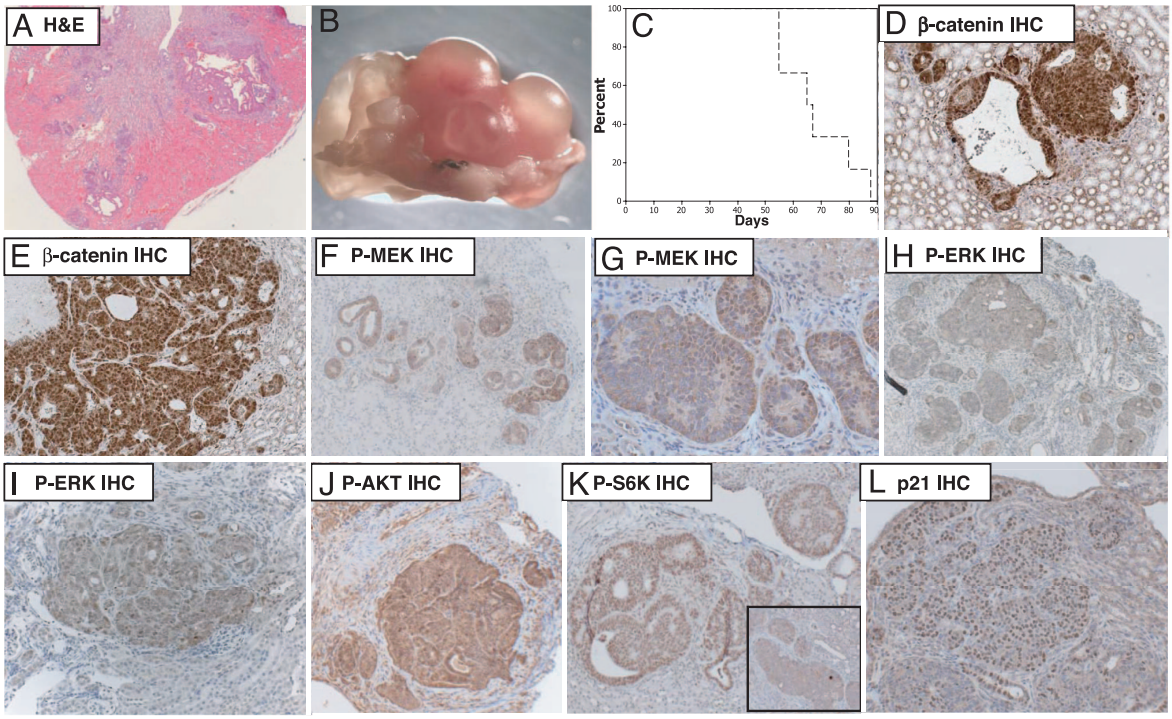

Fig. 3. Oncogenic K-*ras*^{V12} rapidly accelerates renal cell carcinoma caused by Apc deficiency. (*A*) H&E-stained section of kidney from *AhCre*$^{+/T}$, *K*-ras$^{+/LSLV12}$, Apc$^{fl/fl}$ at 2 months of age. Note the presence of multiple kidney lesions. (*B*) Macroscopic image showing grossly altered kidney morphology of *AhCre*$^{+/T}$, K-*ras*$^{+/LSLV12}$, *Apc*$^{fl/fl}$ at 3 months of age. (*C*) Kaplan–Meier curve showing survival of *AhCre*$^{+/T}$, K-*ras*$^{+/LSLV12}$, *Apc*$^{fl/fl}$ (dashed line) and *AhCre*$^{+/T}$, K-*ras*$^{+/+}$, *Apc*$^{fl/fl}$ (solid line) after Cre induction (log rank $P = 0.001$, $n = 10$). All *AhCre*$^{+/T}$, K-*ras*$^{+/LSLV12}$, *Apc*$^{fl/fl}$ had to be culled by 4 months of age because of kidney tumor burden. At this stage no *AhCre*$^{+/T}$, K-*ras*$^{+/+}$, *Apc*$^{fl/fl}$ mice showed any overt signs of illness or had developed kidney tumors. (*D* and *E*) β-catenin is up-regulated and relocalized to the nuclei of all kidney lesions of *AhCre*$^{+/T}$, K-*ras*$^{+/LSLV12}$, *Apc*$^{fl/fl}$ mice. (*F* and *G*) Up-regulation of cytoplasmic P-MEK, which was observed in all kidney lesions. (*H* and *I*) Up-regulation of P-ERK 1/2, again observed in all kidney lesions of *AhCre*$^{+/T}$, K-*ras*$^{+/LSLV12}$, *Apc*$^{fl/fl}$ mice. (*J*) Up-regulation of P-Akt in kidney lesions arising in *AhCre*$^{+/T}$, K-*ras*$^{+/LSLV12}$, *Apc*$^{fl/fl}$ mice. (*K*) Nuclear P-S6 kinase in kidney lesions arising in *AhCre*$^{+/T}$, K-*ras*$^{+/LSLV12}$, *Apc*$^{fl/fl}$. (*Inset*) Up-regulation of P-mTOR in the kidney lesions. (*L*) Up-regulation of p21 in kidney lesions arising in *AhCre*$^{+/T}$, K-*ras*$^{+/LSLV12}$, *Apc*$^{fl/fl}$ mice. (Magnifications: *A*, ×40; *B–L*, ×400.)

studies *in vivo* in both the colon and lung had failed to see dysregulation of these pathways after K-*ras* oncogene expression, even within tumors (9, 12). Although we did not see gross activation of Raf-MEK-ERK signaling in all intestinal adenomas, we did observe higher levels of P-MEK and occasional nuclei positive for P-ERK in a proportion of the small intestinal adenomas (≈10%) arising in *AhCre*$^{+/T}$, *K-ras*$^{+/LSLV12}$, *Apc*$^{+/fl}$ mice. Similar changes were not observed in the *AhCre*$^{+/T}$, *K-ras*$^{+/+}$, *Apc*$^{+/fl}$ cohort. There was also no gross activation of the Akt signaling pathways with similar patterns and levels of expression of P-Akt$^{Ser\text{-}473}$ and its downstream effectors mTor$^{Ser\text{-}2448}$ and S6 kinase$^{Thr\text{-}421,Ser\text{-}424}$ (data not shown). These data suggest either that relatively low-level activation of the Raf-MEK-ERK pathway is sufficient to mediate the effects of the K-*ras*^{V12} oncogene or that alternate pathways are responsible.

The K-*ras*^{V12} Oncogene Accelerates RC with Concomitant Activation of Raf-MEK-ERK and Akt Signaling Pathways. The *AhCre* transgene also drives constitutive expression of Cre recombinase in the renal epithelium without causing *Apc* loss in the intestine. This property has been used to drive homozygous deletion of *Apc* in *AhCre*$^{+}$, *Apc*$^{fl/fl}$ animals. Indeed, these mice spontaneously develop RC with an incidence of 30% at 12 months at age. These tumors invariably display loss of both *Apc* alleles. The relative low frequency of tumors, despite high levels of Cre-mediated recombination, appears to reflect spontaneous deletion of the majority of Apc-deficient cells in a p53-dependent manner (22).

To investigate whether expression of the K-*ras*^{V12} oncogene accelerates RC in these mice, we first examined kidneys from (*AhCre*$^{+/T}$, *K-ras*$^{+/+}$, *Apc*$^{+/+}$), (*AhCre*$^{+/T}$, *K-ras*$^{+/LSLV12}$, *Apc*$^{+/+}$), (*AhCre*$^{+/T}$, *K-ras*$^{+/+}$, *Apc*$^{fl/fl}$), and (*AhCre*$^{+/T}$, *K-ras*$^{+/LSLV12}$, *Apc*$^{fl/fl}$) mice at 2 months of age ($n = 12$). At this time point no lesions were found in (*AhCre*$^{+/T}$, *K-ras*$^{+/+}$, *Apc*$^{+/+}$), (*AhCre*$^{+/T}$, *K-ras*$^{+/LSLV12}$, *Apc*$^{+/+}$), or (*AhCre*$^{+/T}$, *K-ras*$^{+/+}$, *Apc*$^{fl/fl}$) animals. However, all floxed Apc mice expressing the K-*ras*^{V12} allele (*AhCre*$^{+/T}$, *K-ras*$^{+/LSLV12}$, *Apc*$^{fl/fl}$ mice) were characterized by RC in addition to many smaller lesions (Fig. 3*A*). To further analyze the onset of RC we then aged cohorts of (*AhCre*$^{+/T}$, *K-ras*$^{+/+}$, *Apc*$^{fl/fl}$) and (*AhCre*$^{+/T}$, *K-ras*$^{+/LSLV12}$, *Apc*$^{fl/fl}$) mice ($n = 10$) until they became symptomatic of disease (swollen, blood in urine, anemic). By 4 months of age all double mutant *AhCre*$^{+/T}$, *K-ras*$^{+/LSLV12}$, *Apc*$^{fl/f1}$ animals became ill and were confirmed to have RC (Fig. 3 *B* and *C*). At this time point, no RC was observed in the *AhCre*$^{+/T}$, *K-ras*$^{+/+}$, *Apc*$^{fl/fl}$ cohort. Molecular analysis revealed nuclear β-catenin within every kidney lesion, implying loss of the WT Apc alleles (Fig. 3 *D* and *E*). P21 and cyclin D1 was also up-regulated within most lesions (Fig. 3*L* and data not shown). Critically, we observed up-regulation of P-MEK and nuclear P-ERK, indicating that the Raf-MEK-ERK pathway was activated within these tumors (Fig. 3 *F–I*). We also observed up-regulation of P-Akt$^{Ser\text{-}473}$ and the downstream effectors mTOR^{2448} and S6 kinase$^{Ser\text{-}421/Thr\text{-}424}$ (Fig. 3 *J* and *K*). Up-regulation of Akt signaling and particularly mTOR has previously be associated in RC because of loss of the tuberous sclerosis tumor suppressor genes (*TSC1* or *TSC2*) (23).

The relative lack of lesions in the *AhCre*$^{+/T}$, *K-ras*$^{+/+}$, *Apc*$^{fl/fl}$ mice at these stages suggests that expression of the oncogenic K-*ras*^{V12} allele allows the survival of Apc-deficient cells during the early stages of tumorigenesis. This parallels our previous study where we found p53 deficiency also accelerated tumorigenesis, although this effect was less marked than that observed here. K-*ras*^{V12} expression

is also likely to drive increased lesion growth, as Apc-deficient kidneys are characterized by β-catenin-positive foci at 3 months but these do not progress to RC until many months later (22).

Two previous studies have shown activation of the Raf-MEK-ERK pathways in tumors *in vivo* after endogenous K-*ras* oncogene activation. Notably, one of these studies required coincident loss of PTEN in endometrioid ovarian adenocarcinoma (24). The second study was performed in pancreatic adenocarcinomas after combined expression of an oncogenic K-*ras* allele and loss of p53 (25). Together with the data presented here, these studies argue that both cellular and genetic contexts are critical determinants of the consequences of K-*ras* mutation. The observed differences in renal, pancreatic, and intestinal epithelium may reflect the relatively high levels of P-MEK and P-ERK staining in normal intestinal enterocytes compared with normal renal or pancreatic epithelium. Thus, the effects of K-*ras* mutation may be less aggressive in tissues (such as the intestinal epithelium) in which these pathways are normally activated and where the appropriate feedback loops are expressed. In this light it is of interest to note that within Madin Darby canine kidney cells loss of active ERK/MEK signaling restores cells to an epithelial state (26).

In the intestine, oncogenic K-*ras* expression leads to both accelerated adenoma development and increased invasiveness, but only after *Apc* deficiency. The latter effect is of particular note as one of the immediate phenotypes of *Apc* deficiency is a complete loss of cell migration and coincident up-regulation of proteins such as TIAM1 (27) and the EphB receptors (28). The later stages of colorectal cancer are marked by a progressive deregulation of proteins, including E-Cadherin, and the EphB receptors, which may reverse this consequence of Apc loss and so permit invasion. Our data suggest that expression of oncogenic K-*ras* provides a further mechanism for this reversal (28).

In summary, we have elucidated the consequences of expressing an endogenous K-*ras*^{V12} oncogene in intestinal and renal epithelium. Expression of the K-*ras*^{V12} oncogene in these tissues by itself had no phenotypic consequences. However, *Apc* deficiency makes these cells permissive for the tumorigenic properties of K-*ras* oncogenes. These tissues, however, differ markedly in the specific contributions of K-*ras*^{V12} expression. Whereas the renal epithelium is exquisitely sensitive to the consequences of K-*ras*^{V12} expression in the absence of *Apc*, expression of oncogenic K-*ras*^{V12} in the intestinal epithelium has little or no impact on physiology and does not accentuate the immediate effects of *Apc* deficiency. However, over the long term, oncogenic K-*ras*^{V12} expression accelerates both intestinal adenoma formation and invasion. These data demonstrate distinct tissue-specific responses to K-*ras* oncogenes, differences that may reflect the activation state of the Raf-MEK-ERK pathway in these tissues.

Materials and Methods

Experimental Animals. All procedures were conducted according to U.K. Home Office regulations. Mice were maintained on an outbred background, and all mice were genotyped as described for the targeted Apc^{580s} allele (15), K-*ras*^{V12} allele (10), and the AhCre transgene (13). Cre activity was induced in control and experimental mice by 3 i.p. injections of 80 mg/kg β-naphthoflavone within 24 h (4, 13).

Assaying Crypt Size, Apoptosis, Mitosis, and S-Phase Labeling *in Vivo*. Apoptosis, crypt size, and mitotic index were scored from H&E-stained sections as described (4). For each analysis, 25 full crypts were scored from at least three mice of each genotype. For BrdU labeling, mice were injected either 2 h or 48 h before culling with 0.25 ml of BrdU (Amersham, Piscataway, NJ), and staining was performed using an anti-BrdU antibody (BD, Franklin Lakes, NJ) at 1 part in 100. At least three mice were used for each genotype and time point

β-Gal Analysis. Intestinal whole mounts were prepared, fixed, and exposed to X-Gal substrate by using a method as reported (4).

Histology and IHC. Intestinal tissue was fixed in ice-cold 10% neutral buffered formalin for no longer than 24 h before being processed into paraffin blocks according to standard procedures. Tissue sections (5 μm) were either stained with H&E for histological analysis or used for IHC. The details of the antibodies used are given in *Supporting Text*, which is published as supporting information on the PNAS web site.

RNA Extraction and Affymetrix Microarray Analysis. Eight-week-old male mice were used for the array analysis. Three centimeters of the small intestine located 7 cm from the stomach was placed in RNA*later* (Ambion, Austin, TX) (after removing any mesentery and ensuring that no Peyer's patches were present). The tissue was then homogenized in Trizol reagent, and RNA was extracted by using standard phenol-chloroform methodologies. Biotinylated target cRNA was generated as described (4). Affymetrix (Santa Clara, CA) gene arrays were run at the Cancer Research U.K. facility at the Paterson Institute for Cancer Research. Samples were hybridized to MOE430_2 chips. In total, six chips were used: three for WT intestine and three for K-*ras*^{v12} intestine (each chip represented RNA made from an individual mouse intestine). Raw signal intensities were initially screened by using the MaxD/View program to remove false-positive and false-negative signals (using a cutoff of at least one P value for each transcript < 0.2). The data were then normalized by global normalization, using the MaxD/View-Program (4). qRT-PCR was performed as described in *Supporting Text*.

This work was supported by Cancer Research U.K.

1. Kinzler KW, Vogelstein B (1996) *Cell* 87:159–170.
2. Bienz M, Clevers H (2000) *Cell* 103:311–320.
3. Kinzler KW, Nilbert MC, Su LK, Vogelstein B, Bryan TM, Levy DB, Smith KJ, Preisinger AC, Hedge P, McKechnie D, *et al.* (1991) *Science* 253:661–663.
4. Sansom OJ, Reed KR, Hayes AJ, Ireland H, Brinkmann H, Newton IP, Batlle E, Simon-Assmann P, Clevers H, Nathke IS, *et al.* (2004) *Genes Dev* 18:1385–1390.
5. Malumbres M, Barbacid M (2003) *Nat Rev Cancer* 3:459–65.
6. Pollock CB, Shirasawa S, Sasazuki T, Kolch W, Dhillon AS (2005) *Cancer Res* 65:1244–1250.
7. Janssen KP, el-Marjou F, Pinto D, Sastre X, Rouillard D, Fouquet C, Soussi T, Louvard D, Robine S (2002) *Gastroenterology* 123:492–504.
8. Coopersmith CM, Chandrasekaran C, McNevin MS, Gordon JI (1997) *J Cell Biol* 138:167–179.
9. Johnson L, Mercer K, Greenbaum D, Bronson RT, Crowley D, Tuveson DA, Jacks T (2001) *Nature* 410:1111–1116.
10. Guerra C, Mijimolle N, Dhawahir A, Dubus P, Barradas M, Serrano M, Campuzano V, Barbacid M (2003) *Cancer Cell* 4:111–120.
11. Chan IT, Kutok JL, Williams IR, Cohen S, Kelly L, Shigematsu H, Johnson L, Akashi K, Tuveson DA, Jacks T, Gilliland DG (2004) *J Clin Invest* 113:528–538.
12. Tuveson DA, Shaw AT, Willis NA, Silver DP, Jackson EL, Chang S, Mercer KL, Grochow R, Hock H, Crowley D, *et al.* (2004) *Cancer Cell* 5:375–387.
13. Ireland H, Kemp R, Houghton C, Howard L, Clarke AR, Sansom OJ, Winton DJ (2004) *Gastroenterology* 126:1236–1246.
14. Marshman E, Ottewell PD, Potten CS, Watson AJ (2001) *J Pathol* 195:285–292.
15. Shibata H, Toyama K, Shioya H, Ito M, Hirota M, Hasegawa S, Matsumoto H, Takano H, Akiyama T, Toyoshima K, *et al.* (1997) *Science* 278:120–123.
16. Park KS, Jeon SH, Kim SE, Bahk YY, Holmen SL, Williams BO, Chung KC, Surh YJ, Choi KY (2006) *J Cell Sci* 119:819–827.
17. Li J, Mizukami Y, Zhang X, Jo WS, Chung DC (2005) *Gastroenterology* 128:1907–1918.
18. Kolch W (2005) *Nat Rev Mol Cell Biol* 6:827–837.
19. Cho H, Kozasa T, Bondjers C, Betsholtz C, Kehrl JH (2003) *FASEB J* 17:440–442.
20. Cismowski MJ, Takesono A, Ma C, Lizano JS, Xie X, Fuernkranz H, Lanier SM, Duzic E (1999) *Nat Biotechnol* 17:878–883.
21. Yip-Schneider MT, Lin A, Marshall MS (2001) *Biochem Biophys Res Commun* 280:992–997.
22. Sansom OJ, Reed KR, Griffiths D, Winton DJ, Clarke AR (2005) *Oncogene* 24:8205–8210.
23. Hay N (2005) *Cancer Cell* 8:179–183.
24. Dinulescu DM, Ince TA, Quade BJ, Shafer SA, Crowley D, Jacks T (2005) *Nat Med* 11:63–70.
25. Hingorani SR, Wang L, Multani AS, Combs C, Deramaudt TB, Hruban RH, Rustgi AK, Chang S, Tuveson DA (2005) *Cancer Cell* 7:469–483.
26. Schramek H, Feifel E, Marschitz I, Golochtchapova N, Gstraunthaler G, Montesano R (2003) *Am J Physiol* 285:C652–C661.
27. Malliri A, Rygiel TP, van der Kammen RA, Song JY, Engers R, Hurlstone AF, Clevers H, Collard JG (2006) *J Biol Chem* 281:543–548.
28. Batlle E, Bacani J, Begthel H, Jonkheer S, Gregorieff A, van de Born M, Malats N, Sancho E, Boon E, Pawson T, *et al.* (2005) *Nature* 435:1126–1130.